Australian Journal of Crop Science AJCS
AJCS 6(1):109-115 (2012) ISSN:1835-2707

Retrieval of maize leaf chlorophyll content using peak–valley characteristic parameters from imaging hyperspectra

Dongyan Zhang[1, 2], Jinling Zhao[1], Wenjiang Huang[1], Dazhou Zhu[1], Linsheng Huang[1], Xingang Xu[1], Zhihong Ma[1] and Jihua Wang[1, 2]*

[1]Beijing Research Center for Information Technology in Agriculture, Beijing 100097, China;
[2]Institute of Agricultural Remote Sensing & Information Technology Application, Zhejiang University, Hangzhou 310029, China

***Corresponding author: hello-lion@hotmail.com**

Abstract

In situ hyperspectral imaging has great application potential in crop nutrient determination using high spectral and spatial resolution. To detect chlorophyll content of crop components accurately, imaging and non-imaging spectrometers were simultaneously used to record the reflectance spectra of maize leaves from different layers. The peak–valley characteristic parameters were extracted from the change rates and their derived variables from the spectral curve on the blue, green, yellow, and red edge were then calculated to determine chlorophyll content. By analyzing the correlations between the feature parameters and the leaf chlorophyll concentrations, the feasibility of using these parameters was verified. The results reveal that peak–valley characteristic parameters such as RVA1, Kg/Kr, GPA2/RVA2, and Kb are significantly correlated with chlorophyll content, and among them, the regression coefficient (R^2) of RVA1 was the highest (R^2 = 0.705). Finally, an inverse model (y = 1.282x - 0.143) of chlorophyll content was constructed using RVA1. The R^2 value of the validated model of chlorophyll content was 0.640, and the corresponding root mean square error was 0.3039. These results indicate that estimating chlorophyll content is feasible using peak–valley characteristic parameters extracted from hyperspectral imaging data.

Keywords: Analytical spectral devices; chlorophyll content; maize leaf; pushbroom hyperspectral imaging; peak-valley characteristic parameter.
Abbreviations: ASD-analytical spectral devices; C/N-carbon/nitrogen; CARI-chlorophyll absorption ratio index; DN-digital number; $D\lambda_b$- blue amplitude; $D\lambda_y$- yellow amplitude; $D\lambda_r$-red amplitude; FDR -first order derivative reflectance; GPA1- the included angle specified by the two sides (green edge and yellow edge) of green peak; GPA2- the included angle specified by the two sides (green edge and peak-to-valley edge) of green peak; GPA1/ GPA2, RVA1 /RVA2-Angle ratio; Kb- the rates of change of spectral curve on the blue edge (490~530 nm); Kg- the rates of change of spectral curve on the green edge (500~550 nm); Ky- the rates of change of spectral curve on the yellow edge (550~580 nm); Kpv- the rates of change of spectral curve from the top of green peak to the bottom of red valley (550–670 nm); Kr- the rates of change of spectral curve on the red edge (680~750 nm); Kg/ Kb, Kg/ Ky, Kg/ Kpv, Kg/ Kr, Kr/ Kb, Kr/ Kg, Kr/ Ky, Kr/ Kpv -spectral ratio; PIS-pushbroom hyperspectral imaging; PRI-pigment ratio index; PVCP-peak-valley characteristic parameters; Peak-to-valley edge-the peak-to-valley edge refers to the band range (550–670 nm) from the top of green peak to the bottom of red valley on the visible spectral curve; RMSE -root mean square error; R_{rv}-reflectance of red valley; R_{gp}-reflectance of green peak; R_g/R_{rv}-ratio of green peak and red valley; RVA1- the included angle specified by the two sides (yellow edge and red edge) of red valley; RVA2- the included angle specified by the two sides (peak-to-valley edge and red edge) of red valley; SE- standard error; TVI- triangular vegetation index; λ_b- blue position; λ_y - yellow position; λ_r-red position; λ_{gp}-green position; λ_{rv}-red valley position.

Introduction

The rapid, non-destructive, and accurate determination of crop nutrient status using spectral imaging technology remains a crucial question in agriculture. A large number of studies have been performed to explore the correlations among the ground-based hyperspectral data and the physiologic and biochemical characteristic indicators of crops, such as leaf area, biomass, chlorophyll, nitrogen, C/N ratio, and so on. (Daughtry et al., 2000; Gong et al., 2002; Hansen et al., 2003; Vianney et al., 2007). Among these indicators, chlorophyll is the key indicator of crop photosynthesis and it reflects the level of crop stress. Therefore, it is usually used in the non-destructive monitoring of crop growth status through optical spectrometry (Haboudane et al., 2002; Huang et al., 2004; Bannari et al., 2007; Haboudane et al., 2008; Zhang et al., 2010).Currently, there are two main methods for monitoring crop chlorophyll content. One method uses various spectral indices generated by different band combinations, such as the chlorophyll absorption ratio index (Elvidge et al., 1995), the pigment ratio index (Broge et al., 2000), and the triangular vegetation index (Chen et al., 2010). These methods often use wide-band multispectral imagery data and early hyperspectral applications (Oppelt et al., 2004; Zhang et al., 2010). The other type employs the feature variables defined by changes spectral reflectance. The latter method can be further divided into two forms. One measures

the chlorophyll changes using the reflection spectra or the characteristic values of reflection peaks, and absorption valleys of normalized spectrum, as well as their derivatives (Wang et al., 2010). These methods are used mainly for assessing biological components at the single-leaf scale. For studies at the canopy-scale, impact factors, such as sensor performance (signal to noise ratio and bandwidth) and differences in canopy structure, must be considered (Kokaly et al., 1999). The other is the determination of chlorophyll content based on the characteristics of its derivative spectrum and their transformational forms. Considering the derivative spectrum can accurately determine the inflection points and extreme value of the spectral change regions such as the blue edge, yellow edge, and red edge, it is much more relevant in vegetation (Adams et al., 1999; Cho et al., 2006). In recent years, the emergence of narrow-band hyperspectral data allows the analysis of the variations in chlorophyll concentration based on characteristic shapes between the peaks and valleys of spectral reflectance, such as the characteristic location, peak height or width, and the area of valley depth, as well as their derived variables (Pu et al., 2009). Hyperspectral imaging technology provides more information, it is faster and non-destructive, and it can be done in real-time unlike non-imaging sensors. By combining imaging with spectroscopy, it can study not only group-scale crops, but also microscopic individuals and components. Therefore, hyperspectral imaging technology provides the essential technical and equipment support for probing the features of group and individuals and their metabolism (Tong et al., 2010). However, utilizing the strengths of imaging hyperspectral data requires sophisticated data mining techniques (Ye et al., 2008). The current study focuses on finding better parameters for assessing chlorophyll concentration through peak–valley characteristic variables such as the rising and falling rates of peak–valleys and angles derived from the both sides of peaks, and valleys from imaging spectra. In addition, comparison and analysis of differences in peak–valley characteristic parameters were calculated from data from imaging and non-imaging spectrometry. Hyperspectral imaging data was proven practical.

Results

Feasibility Analysis for Extracting Characteristic Parameters from Imaging Hyperspectra

The results from a previous study indicated that the non imaging hyperspectra could effectively improve the capability of estimating barley canopy chlorophyll concentration using novel characteristic parameters, such as the change in the rates of the blue, green, and yellow edges and their derived variables (Xu et al., 2011). However, the usefulness of this approach has not been validated. Consequently, the reflectance of corn leaves from different layers (Fig. 3) was determined to verify the possibility in the leaf-scale for peak-valley characteristic parameters, and to identify optimal methods for accurately determining the chlorophyll content of maize leaves using hyperspectral imaging data. As shown in Fig. 3a, obvious differences in the spectral values were evident among the leaves from different layers at the bell-mouthed period. The first leaves had the highest reflectance at 550 nm (green peak position), followed by the second, the fourth, and the third leaves. Little spectral differences were observed between the third and the fourth leaves. At 670 nm (red valley position), little spectral differences were observed between the first and the second leaves, which was similar to that observed between the third and the fourth leaves. Visually, the leaf reflectance curves displayed two layers. For the red edge range (670 nm to 750 nm), the red edges of the first and second leaves were close to the green peak position, and those of the third and the fourth leaves tended to the far red. The corresponding chlorophyll content in the leaves from different layers were 0.7 mg/g, 0.9 mg/g, 1.4 mg/g, and 1.5 mg/g, respectively, which indicated that the leaves with low chlorophyll content exhibited strong reflectance in the green peak position and the leaves with high chlorophyll content had strong absorbance in the red valley position. These findings served as the basis for determining the differences in crop nutrients based on spectroscopy. In principle, peak–valley characteristic parameters can be extracted from the imaging spectral data. Meanwhile, considering the high accuracy of monitoring crop leaf nutrients using the ASD integrating sphere, it was used to collect leaf spectral information, as shown in Fig. 3b. The leaf spectra from the different layers had similar curves compared with the imaging spectral data, which suggests that hyperspectral imaging data are more accurate.

Correlation Relationship between Chlorophyll Content and Hyperspectral Characteristic Parameters

Chlorophyll content is a good indicator for crop growth and development, therefore, accurately determining and assess chlorophyll concentration is essential (Bannari et al., 2007). The current study extracted peak–valley characteristic parameters and determined their correlations with chlorophyll content by analyzing the characteristics of hyperspectral curves. Furthermore, comparative analysis was performed for the correlations between the peak–valley parameters and the traditional three-edge parameters to verify the accuracy of the peak–valley parameters in estimating chlorophyll content (Table 4). As shown in Table 4, the correlations were extremely significant between the peak–valley characteristic parameters and the chlorophyll content apart from those with Kr, RVA2, and GPA1/RVA1. However, only Dλb, Dλy, Rg, λr, and λrv were markedly related to the traditional feature variables. Among them, Kb, Kg, Kg/Kr, RVA1, and GPA2/RVA2 had good correlation coefficients ($r > 0.7$). In contrast, Dλb, Rg, and λr were the only traditional three-edge parameters that had correlation coefficients greater than 0.7. This suggests that the peak–valley characteristic parameters, which were derived using three-edge spectral change rate, significantly improved the predictability of chlorophyll concentration. Both the peak–valley and traditional parameters were based on three-edge technology; most of them were calculated using the first order differential of the original spectra. However, the high correlation of the peak–valley parameters might be because the spectral information for quantitative components of crop was displayed in the form of overall characteristic ranges rather than a single individual point. The peak–valley parameters corresponded solely to this feature, which used region change rates for construction; thus, they might be a more comprehensive response to the variations in crop components than a single point. Secondly, single-point spectra possibly had greater errors caused by the instrument, light illumination, data processing methods, and so on. Fig. 4 shows the first order derivative reflectance (FDR) for the same leaves between the imaging and non-imaging data. Although they share the same change trends, the performance of single point exhibit different spectral characteristics. Therefore, to determine the crop component information accurately, all sensitive bands in the entire region must be integrated to avoid the effect of baseline drift. In addition, the current study used non-imaging hyperspectral data to verify the practicality of using peak–valley characteristic parameters (Table 5). Among these parameters, the correlation coefficients of the peak–valley characteristic parameters,

Table 1. The key performance parameters of imaging and non-imaging spectrometers

Performance parameters	PIS	ASD
Spectrum range	400 nm to 1000 nm	350 nm to 1000 nm
Spectrum resolution	2 nm	3 nm
Sampling interval	0.7 nm	1.4 nm
FOV	16°	25°
Spatial resolution	0.5 mm	
Pixel dimension	7.4 μm × 7.4 μm	
Image resolution	1400 (Spatial) × 1024 (Spectral)	

Table 2. The traditional characteristic parameters

Name	Characteristic parameter
Blue edge	Blue amplitude ($D\lambda_b$), blue position(λ_b)
Yellow edge	Yellow amplitude ($D\lambda_y$), yellow position (λ_y)
Red edge	Red amplitude ($D\lambda_r$), Red position (λ_r)
Green peak	Reflectance of green peak (R_{gp}) and green position (λ_{gp})
Red valley	Reflectance of the red valley (R_{rv}) and the red valley position (λ_{rv})
Ratio of the Green peak to the Red valley	R_g/R_{rv}

Table 3. Description of peak-valley spectral characteristic parameters

Name	Definition
Kb	The rates of change in the spectral curve on the blue edge (490 nm to 530 nm)
Kg	The rates of change in the spectral curve on the green edge (500 nm to 550 nm)
Ky	The rates of change in the spectral curve on the yellow edge (550 nm to 580 nm)
Kpv	The rates of change in the spectral curve from the top of the green peak to the bottom of the red valley (550 nm to 670 nm)
Kr	The rates of change in the spectral curve on the red edge (680 nm to 750 nm)
GPA1	The included angle specified by the two sides (green edge and yellow edge) of the green peak
GPA2	The included angle specified by the two sides (green edge and peak-to-valley edge) of the green peak
RVA1	The included angle specified by the two sides (yellow edge and red edge) of the red valley
RVA2	The included angle specified by the two sides (peak-to-valley edge and red edge) of the red valley
	Derivative variable
Spectral ratio	Kg/Kb, Kg/Ky, Kg/Kpv, Kg/Kr, Kr/Kb, Kr/Kg, Kr/Ky, Kr/Kpv
Angle ratio	GPA1/GPA2, RVA1/RVA2

Notes: The peak-to-valley edge refers to the band range (550 nm to 670 nm) from the top of green peak to the bottom of red valley on the visible spectral curve.

including Kg, Kg/Kr, RVA1, and GPA2/RVA2 all reached 0.71 and the highest value was 0.791, whereas only the coefficients of Dλb, Rg, and λr exceeded 0.71 and the largest value was 0.786. As shown in the analysis above, the results measured by two instruments indicate that peak–valley characteristic parameters were more suitable for estimating chlorophyll content. However, although the same parameters were selected for imaging and non-imaging data, the correlation coefficients were different. For the peak–valley characteristic parameters from the imaging data, the order of the correlation coefficients was RVA1 > Kg/Kr > GPA2/RVA2 > Kb, whereas the result of non-imaging data was Kb > Kg/Kr > Kg > RVA1 > GPA2/RVA2. For the traditional characteristic parameters from the imaging data, the order of the parameters was λr > Dλb > Rg, whereas that of non-imaging data was λr > Rg > Dλb. The above differences combined with those in Fig. 4 can be explained by the following: (1) The difference in the spectral interval, which was 0.7 nm for the imaging data and 1 nm for the non-imaging data, indicates the effect of spectral interval on the results. (2) For the imaging data, the value was derived from the average spectra of the entire leaf, whereas the value was derived from the average spectra of several points on a leaf using the non-imaging data; this suggests some differences in reflecting the inner components of the leaves. (3) The area spectrum is more easily affected by light compared with the point spectra, which was likely induced by different instruments, (4) Before the non-imaging data was used, they had been optimized by its own software, but the imaging data were just processed step by step using the five-point average method.

Constructing and Validating Model of Retrieving Leaf Chlorophyll Content Using Peak-Valley Characteristic Parameters

Based on the correlations between the peak–valley characteristic parameters and the chlorophyll concentration, the optimal characteristic parameter was chosen to construct a model for estimating chlorophyll content (Fig. 5a) according to the R^2 value and standard error (SE) (Table 6). The results show that the R^2 value between RVA1 and chlorophyll content was the highest and the SE was the least. Therefore, it was used to build the model. In addition, both Kg/Kr and GPA2/RVA2 had high R^2 values and low SEs, indicating that the combined and transformed characteristic parameters reflect the inner components of crops better than single variables. This phenomenon is consistent with the principle that multi-band composite vegetation indices are usually more reliable than single variables in reflecting crop growth status (Haboudane et al., 2002). Given the vertical gradient variance of crop nutrient distribution, only the first and fourth leaves were used to construct the model to increase the contrast. Therefore, the predicted values were concentrated around 0.29 and 0.37 (Fig. 5a). As shown in Fig.5b, the correlation between RVA1 and the chlorophyll concentration was evident; thus, it was used to construct a model for retrieving chlorophyll concentration. Finally, the correction between the predicted values and observed values was established. The R^2 was 0.640 and RMSE was 0.3039, suggesting that assessing leaf-scale component information is feasible using peak–valley characteristic parameters.

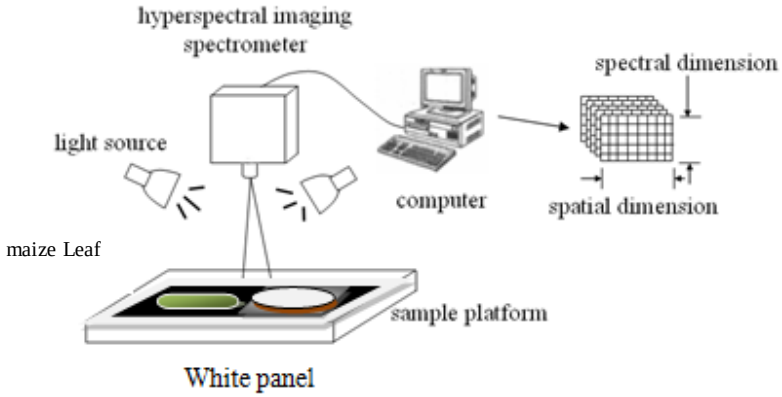

Fig 1. The acquisition system of hyperspectral imaging.

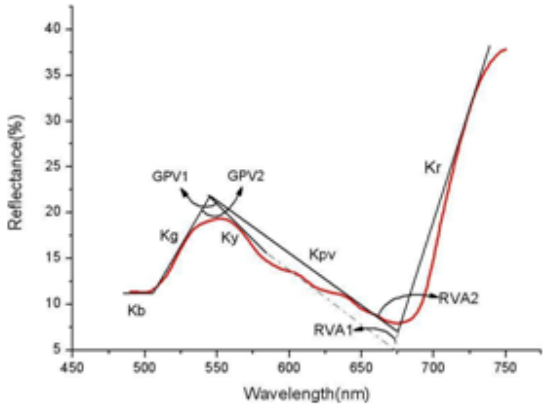

Fig 2. Constitution of peak-valley spectra characteristics parameters.

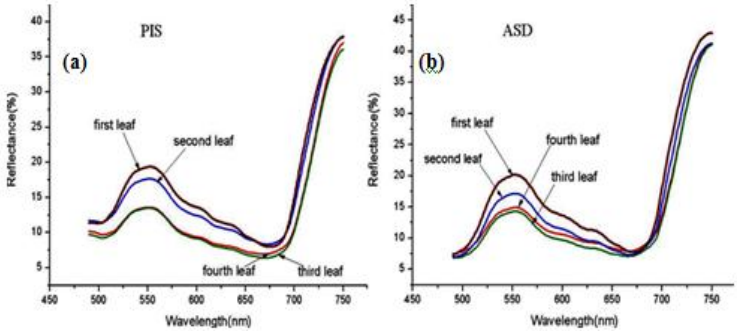

Fig 3. Spectral reflectance curves of leaves from different layers using PIS and ASD

Discussion

The peak–valley characteristic parameters were first proposed by Xu et al. (2011) and it used non-imaging hyperspectral data to estimate the chlorophyll content of barley at the canopy scale. The results showed that new method was suitable for reflecting the growth status of barley. However, the paper did not determine the differences between novel characteristic parameters and traditional feature variables that form spectral curves on the blue, green, and red edge. In addition, the author did not provide more information on whether the novel characteristic parameters have better application effects in other crops and different hyperspectral data. In the current study, the peak–valley characteristic parameters extracted from imaging and hyperspectral data were used to assess the chlorophyll content of maize leaves; the results revealed that the novel means were better than the traditional feature variables. Meanwhile, similar results were achieved by applying non-imaging hyperspectral data in the current study. The results can be explained by the special wavelengths, which are defined as the spectral location that corresponds to the maximum position of the first derivative from reflectance spectra (Lamb et al., 2002; Huang et al., 2004; Yao et al., 2010). These values were indicated by the traditional feature variables, but the novel characteristic parameters reflected the changes from a specific region of spectral reflectance as a key factor, thereby preventing abnormal spectral values of certain single wavelengths to affect the results. Therefore, the new method is better than the traditional means. Imaging hyperspectral spectrometers have a narrower spectral band (0.7 nm) and a higher spectral resolution (2 nm) than those of the spectral band (1 nm) and the non-imaging spectrometer (3 nm) (Table 1). Therefore, methods that are more suitable for emphasizing and exploiting the advantage of imaging hyperspectral data should be found. The results from current research revealed that peak–valley characteristic parameters are more suitable for imaging hyperspectral data. In the future, this method should be extended to canopy nutrition determination for different crops in different growth stages.

Materials and methods

Experimental design

Field experiment was performed at an experimental station affiliated the Beijing Academy of Agricultural and Forestry Sciences (39° 56′ N, 116° 17′ E) in August and October in 2009. Maize variety ZD 958 was selected as the experimental subjects. The corresponding seeds were planted in a field and their general managements were the same as that of locally grown plants. When the corn reached the early bell-mouthed period, the first, second, third leaf, and fourth leaves were collected and were used for determining spectral reflectance using imaging and non-imaging spectrometers in the laboratory.

Data collection and preprocessing

Introduction to imaging and non-imaging spectrometers

The pushbroom hyperspectral imaging spectrometer (PIS) used in the current study was jointly developed by the Beijing Research Center for Information Technology in Agriculture and the University of Science and Technology of China, which acquired images via a linear array push-broom, as shown in Fig.1. Before utilizing PIS for studying the spectral features of objectives, strict laboratory calibration was performed to determine the location of each channel, radiometric accuracy, and so on by the spectrometer designer. The key performance parameters are listed in Table 1. The non-imaging spectrometer used in the study was the ASD Field Spectroradiometer Pro FR 2500 (Analytical Spectral Devices, Inc., Boulder, Colorado, USA).

Table 4. Correlation coefficients between chlorophyll content and characteristic parameters for PIS (n = 84).

PVCP	Correlation coefficient (r)	PVCP	Correlation coefficient (r)	CCP	Correlation coefficient (r)
Kb	-0.723	Kr/Ky	-0.522	Dλb	-0.713
Kg	-0.701	Kg/Kpv	0.606	Dλy	0.620
Ky	0.561	Kr/Kpv	-0.677	Dλr	-0.310
Kpv	0.688	GPA1	0.495	Rg	-0.702
Kr	0.223	GPA2	-0.689	Rrv	-0.441
Kg/Kb	0.614	RVA1	0.792	λb	0.432
Kg/Ky	0.727	RVA2	-0.306	λy	-0.274
Kg/Kr	-0.741	GPA1/RVA1	-0.331	λr	0.715
Kr/Kb	0.561	GPA2/RVA2	-0.726	λg	-0.320
Kr/Kg	0.635	Rg/Rrv	-0.472	λrv	-0.606

Notes: for $p > 0.05$, $r = 0.3126$; for $p > 0.01$, $r = 0.4732$. PVCP meant peak–valley characteristic parameters; CCP meant conventional characteristic parameters.

Table 5. Correlation coefficients between chlorophyll content and characteristic parameters for ASD (n = 84).

PVCP	Correlation coefficients (r)	PVCP	Correlation coefficients (r)	CCP	Correlation coefficients (r)
Kb	-0.791	Kr/Ky	-0.202	Dλb	-0.738
Kg	-0.761	Kg/Kpv	0.247	Dλy	0.567
Ky	0.536	Kr/Kpv	-0.170	Dλr	-0.456
Kpv	0.621	GPA1	0.235	Rg	-0.748
Kr	-0.219	GPA2	-0.711	Rrv	-0.241
Kg/Kb	0.557	RVA1	0.757	λb	0.270
Kg/Ky	0.410	RVA2	-0.443	λy	-0.171
Kg/Kr	-0.767	GPA1/RVA1	-0.202	λr	0.786
Kr/Kb	0.626	GPA2/RVA2	-0.714	λg	-0.256
Kr/Kg	0.539	Rg/Rrv	-0.632	λrv	-0.447

Notes: $r = 0.3126$ ($p > 0.05$), $r = 0.4732$ ($p > 0.01$). PVCP meant peak–valley characteristic parameters; CCP meant conventional characteristic parameters.

Table 6. Statistics of formulas, R^2 and SE between feature parameters and chlorophyll content.

Feature parameters	Regression equation	R^2	SE
RVA1	y = 1.282x- 0.143	0.705	0.034
Kg/Kr	y = -0.654x + 0.466	0.640	0.044
GPA2/RVA2	y = -0.572x + 0.497	0.629	0.045
Kb	y = -1.160x + 0.399	0.623	0.045
Kg	y = -1.199x + 0.456	0.606	0.046

The performance parameters from 350 nm to 1000 nm are listed in Table 1. In the current study, the ASD data were interpolated into 1 nm from 400 nm to 1000 nm.

Hyperspectral data acquisition and processing

Before the experiment was performed, the PIS was fixed at an optimal height, which was only100 cm from the lens to leaves (as shown in Fig.1). To reduce the effects of illumination, two halogen light sources were used symmetrically at a 45° angles. When the imaging cubes were acquired, the maize leaves were placed on a platform with black cloth and moved at a constant speed. In addition, three reference targets, a white panel (high reflectance), a gray cloth (medium reflectance), and a black cloth (low reflectance), with known calibrated spectral reflectance were also measured as references for calculating leaf reflectance, as detailed by Zhang et al.(2011). Simultaneously, non-imaging spectral data were recorded using ASD combined with a LI-COR 1800-12 integrating sphere. The spectral reflectance of the PIS can be obtained through the experiential straight-line method using the following formula:

$$\rho = a \cdot DN + b \quad (1)$$

where a is the mean coefficient; b is the intercept; ρ is the targets reflectance; and DN is the digital number of targets.

Coefficients a and b were regressed using the least square method from the spectral values of the white reference panel, gray cloth, black cloth and their corresponding DNs of images, and were then applied to obtain the spectral reflectance of the targets combined with their DNs. The reflectance of ASD was calculated using the following formula:

$$R_t = \frac{Rad_t}{Rad_r} \times R_r \quad (2)$$

where R_t denotes the target spectral reflectance with the white panel as reference, Rad_t denotes the target radiance acquired by the ASD spectrometer, Rad_r denotes the radiance of the white panel acquired by ASD, and R_r is the reflectance of the reference white panel. In the current study, reflectance was multiplied by 100.

Conventional Characteristic Parameters

The traditional characteristic parameters including blue, yellow, and red edges are shown in Table 2, and their specific definitions can be obtained from a previous study (Li et al., 2010).

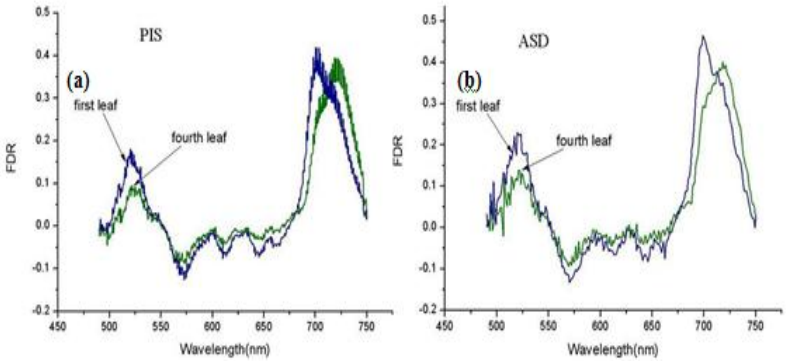

Fig 4. FDR of spectral reflectance of leaves from different layers for PIS and ASD.

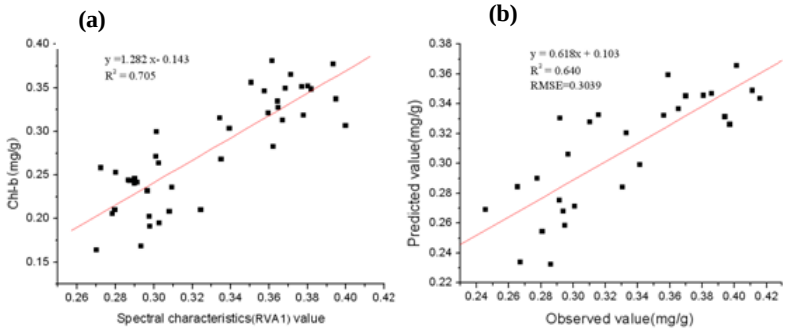

Fig 5 . (a) Predicted model of chlorophyll content (n = 42), **(b)** Validated model of chlorophyll content (n = 28)

Peak-Valley Characteristic Parameters

Peak–valley characteristic parameters were constructed according to the changes in the peaks and valleys of the spectral curves (Fig. 2). By fitting the rate of increase of the blue, green, and red edges and the rate of decrease of the yellow edge, the corresponding slopes were calculated into Kb, Kg, Ky, Kpv, and Kr (Table 3). Additionally, the included angles were specified in terms of the reflectance peaks and absorption valleys of the spectral curves (Table 3). Their specific definitions have been explained by Xu et al. (2011).

Measuring Pigment Content

After measuring the corn leaf spectra, the middle part of leaves (0.5 g) were immediately cut and soaked in 80% acetone solution. The absorbance values of the acetone solution were then measured at 663 nm, 645 nm, and 440 nm using a spectrophotometer. Finally, the concentrations of chlorophyll a, chlorophyll b and chlorophyll a + b were calculated using the extinction coefficient at the corresponding wavelength.

Conclusion

The current study extracted peak–valley and traditional three-edge parameters using imaging spectral data, and then evaluated their abilities to determine chlorophyll content using two methods. The accuracy was then verified using typical non-imaging spectral data. The conclusions were as follows:
(1) The use of peak–valley characteristic parameters extracted from imaging spectral data is feasible.
(2) Compared with the traditional three-edge characteristic parameters, peak–valley parameters have improved ability to reflect chlorophyll content.
(3) The characteristic parameters, including RVA1, Kg/ Kr, GPA2/RVA2, and Kb have higher R^2 values, and RVA1 most accurately reflected chlorophyll content. Finally, the R^2 value of the constructed model was 0.705, and the R^2 value of the validated model was 0.640, with an RMSE value of 0.3039.

Acknowledgments

This work was subsidized by the China Special Funds for Major State Basic Research (Project Number: 2011CB311806), and National Natural Science Foundation of China (Project Number: 41071228, 41071276).

References

Adams M L, Philpot W D, Norvell W A (1999) Yellowness index: an application of spectral derivatives to estimate chlorosis of leaves in stressed vegetation. Int J of Remote Sens 20: 3663-3675

Bannari A, Khurshid K S, Staenz K (2007) A comparison of hyperspectral chlorophyll indices for wheat crop chlorophyll content estimation using laboratory reflectance measurements. IEEE T Geosci Remote Sens 45: 3063-3073

Broge N H, Leblanc E (2000) Comparing prediction power and stability of broadband and hyperspectral vegetation indices for estimation of green leaf area index and canopy chlorophyll density. Remote Sens Environ 76: 156-172

Chen P F, Haboudane D, Tremblay N (2010) A New spectral indicator assessing the efficiency of crop nitrogen treatment in corn and wheat. Remote Sens. Environ. 114: 1987-1997

Cho M A, Skidmore A K (2006) A new technique for extracting the red edge position from hyperspectral data: the linear extrapolation method. Remote Sens Environ 101: 181-193

Daughtry C S T, Walthall C L, Kim M S, Brown D (2000) Estimating corn leaf chlorophyll concentration from leaf and canopy reflectance. Remote Sens Environ 74: 229-239

Elvidge C D, Chen Z (1995) Comparison of broad-band and narrow-band red and near-infrared vegetation indices. Remote Sens Environ 54: 38-48

Gong P, Pu R L, Heald R C (2002) Analysis of in situ hyperspectral data for nutrient estimation of giant sequoia. Int J Remote Sens 23: 1827-1850

Haboudane D, Miller J R, Tremblay N (2002) Integrated narrow-band vegetation indices for prediction of crop chlorophyll content for application to precision agriculture. Remote Sens Environ 81: 416-426

Haboudane D, Tremblay N, Miller J R (2008) Remote estimation of crop chlorophyll content using spectral indices derived from hyperspecral data. IEEE T Geosci Remote Sens 46: 423-427

Hansen P M, Schjoerring J K (2003) Reflectance measurement of canopy biomass and nitrogen status in wheat crops using normalized difference vegetation indices and partial least squares regression. Remote Sens Environ 86: 542-553

Huang W J, Wang J H, Wang Z J (2004) Inversion of foliar biochemical parameters at various physiological stages and grain quality indicators of winter wheat with canopy reflectance. Int J of Remote Sens 25: 2409-2419

Kokaly R F, Clark R N (1999) Spectroscopic determination of leaf biochemistry using band-depth analysis of absorption features and stepwise multiple linear regression. Remote Sens Environ 76: 267-287

Li B Z, Li M X, Zhou X (2010) Hyperspectral estimation models for nitrogen contents of apple leaves. Int J of Remote Sens 14: 767-780

Lamb D W, Steyn-Ross M, Schaare P (2002) Estimating leaf nitrogen concentration in ryegrass pasture using the chlorophyll red edge: Theoretical modeling and experimental observations. Int J of Remote Sens 23: 3619-3648

Oppelt N, Mauser W (2004) Hyperspectral monitoring of physiological parameters of wheat during a vegetation period using AVIS data. Int J of Remote Sens 25: 145-159

Pu R L (2009) Broadleaf species recognition with in situ hyperspectral data. Int J of Remote Sens 30: 2759-2779

Tong Q X, Xue Y Q, Wang J N (2011) Development and application of the field imaging spectrometer system. J of Remote Sens. 14: 409-422

Wang P, Liu X N, Huang F (2010) Retrieval model for subtle variation of contamination stressed maize chlorophyll using hyperspectral data. Spectrosc Spect Analysis 30: 197-201

Xu X G, Zhao C J, Wang J H (2010) Study on relationship between new characteristic parameters of spectral curve and chlorophyll content for rice. Spectrosc Spect Analysis 31: 188-191

Yao X, Tian Y C, Liu X J (2010) Comparative study on monitoring canopy leaf nitrogen status red edge position with different algorithms in wheat. Sci Agri Sin 43: 2661-2667

Vianney H, Martine G, Bruno M (2007) Elaboration of a nitrogen nutrition indicator for winter wheat based on leaf area index and chlorophyll content for making nitrogen recommendations. Eur J Agron27: 1-11

Ye X J, Sakai K, Okamoto H (2008) A ground-based hyperspectral imaging system for characterizing vegetation spectral features. Comput and Electro Agri. 63: 13-21

Zhang D Y, Liu R Y, Song X Y (2010) A field-based pushbroom imaging spectrometer for estimating chlorophyll content of maize. Spectrosc. Spect. Analysis. 31: 771-775

Zhang J H, Chao H, Li D P (2010) Investigation of sulfur dioxide influence on canopy spectral characteristics at early growth stage of rice. Aust J Agric Eng.1:38-44

Zhang D.Y, Zhang J C, Zhu D Z (2011) Investigation of the hyperspectral image characteristics for wheat leaves under different stress. Spectrosc Spect Analysis. 31: 1101-1105